acta physica slovaca vol. 50 No. 1, 267 – 274 February 2000

DISTRIBUTION OF GAMMA RAY FLUXES AT ALTITUDE 500 KM: CORONAS-I DATA

R. Bučík[1,2], K. Kudela[1], A.V. Bogomolov[3], I.N. Myagkova[3], S.N. Kuznetsov[3], S.P. Ryumin[3]

[1] *Institute of Experimental Physics, Slovak Academy of Sciences, 043 53 Košice, Slovakia*
[2] *Technical University in Zvolen, 960 53 Zvolen, Slovakia*
[3] *D.V. Skobel'tsyn Institute of Nuclear Physics, Moscow State University, 119899 Moscow, Russia*

Received 7 October 1998, in final form 30 November 1999, accepted 3 January 2000

Results of the statistical study of gamma ray fluxes in the energy channels 0.12 - 0.32 MeV, 3.0 - 8.3 MeV, measured by the instrument SONG on board the low altitude high inclination satellite CORONAS-I are presented. The geographic maps based on sets of data in March - June 1994 are constructed as well as latitudinal distribution (i.e. the variation of average fluxes with vertical cut - off rigidity) for higher energies is given. The irregular spatial structures of gamma ray flux increases in subauroral zone and at lower latitudes are discussed.

PACS: 95.85.Pw, 94.20.Yx

1 Introduction

Although there exist several earlier measurements of gamma ray flux at low altitudes [1-9] there are not numerous extensive statistical studies revealing the features of the gamma ray flux distribution at altitudes 500-km.

Gamma rays observed in the near-Earth space experiments are superposition of atmospheric gamma rays, local and induced gamma rays produced in the interaction of primary and secondary cosmic rays, the Van Allen radiation, or solar cosmic rays with the material of the instrument and satellite, and diffuse cosmic gamma rays. Atmospheric gamma rays are produced by interactions of cosmic ray protons, alpha particles, and electrons with oxygen and nitrogen nuclei in the atmosphere. At higher energies, gamma rays are created mainly by the decay of π° mesons from high energy nuclear interactions, while at lower energies the gamma rays are produced primarily by bremsstrahlung of primary, secondary and reentrant electrons [10].

The study of spatial distribution of gamma rays at low altitudes is important to test the models for the production of gamma rays in Earth's environment and for understanding of dynamics of the Earth's radiation belts. Such measurements contribute to the construction of radiation models in Earth's magnetosphere. In addition, observed gamma ray fluxes are a background that must be subtracted in near-Earth satellite observations to obtain the gamma ray fluxes from solar energetic emission or others celestial objects in this and similar experiments.

In this paper, we present geographic distribution of average fluxes of gamma rays within period of three months.

2 Experiment

Low altitude satellite CORONAS-I has been devoted to study of various aspects of solar activity. SONG device is a part of the complex measuring high energy electromagnetic and corpuscular emissions from the Sun. Energetic particles are detected by CsI(Tl) crystal scintillator with diameter 20 cm and thickness 10 cm viewed by three photomultipliers, surrounded by the magnetic shielding. The whole scintillator counter is placed under 4π-anticoincidence shielding against charged particles. The shielding is made of plastic scintillator 2 cm thick and consists of two parts. The lower one protects the CsI from below and from the sides and is viewed by one photomultiplier. The upper part is thick, situated in front of CsI and is viewed by two photomultipliers through the light conductors. More details are in Baláž et al., 1994 [11]. CORONAS-I satellite has been launched on March 2, 1994 onto nearly circular orbit with altitude 500 km and inclination $I = 83°$. SONG device was placed on the platform for the scientific instruments separated by about 1 m from the upper end of the satellite body. The nominal orientation during its first working period (until July 5, 1994) was its longitudinal axis has been directed toward the Sun. This was valid for both daily as well as night passes (SONG oriented towards the Earth on night side).

Here we are analyzing the monitoring mode of measurement with 2.5-sec resolution in two (lowest and highest energies) out of four energy channels measuring the gamma rays by SONG instrument.

3 Data set

The data set analyzed in this paper was collected over the period from March 1994 through June 1994. The extent of the set is 1.8×10^6 data points with the time resolution 2.5 s. For the following analysis two energy intervals of gamma rays have been selected, namely $E_A = 0.12 - 0.32$ MeV, and $E_B = 3.0 - 8.3$ MeV. Similar approach for no such extensive statistics of measurements is done in Bučík et al., 1999 [12]. The data have been divided into pixels according to the geographic coordinates with the step of $1°$ in latitude and of $2°$ in longitude. The average number of points of measurements covering one individual pixel is 60. The total data coverage is displayed in Fig. 1. The missing data area over eastern Europe is related with region of data receiving. For each of these pixels the estimate of the mean and dispersion have been evaluated assuming normal distribution of the measurement points. It should be noted this is the zeroth approach suitable for a rough description of flux distribution. The chi-square test of the normality of distribution did not confirm unambiguously for each pixel the normality of the distribution. There are at least two effects influencing the inhomogeneity of the distribution, namely a - the temporal variability, especially at high latitudes due to the variations in flux of high energy electrons precipitating into the atmosphere, and b - the changes in the orientation of the detector (not for all passes at given pixel the orientation with respect to magnetic field is identical).

A correction of the flux of gamma rays was done on daily basis adjusting its absolute value to the ratio of average primary cosmic rays measured by a high cut-off rigidity neutron monitor station Haleakala, and of high energy measurements by SONG instrument (channel measuring protons $E_p > 70$ MeV, and electrons $E_e > 55$ MeV) at low latitudes, namely $L = 1.05$, where L is the McIlwain's parameter (for dipole approximation $\cos^2 \Lambda = L^{-1}$ at the earth's surface, Λ

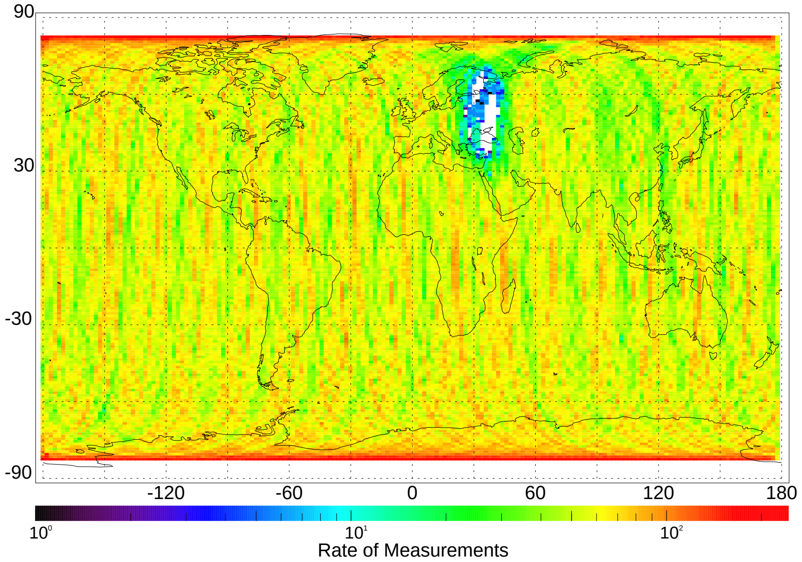

Fig. 1. The map of measurements covering by SONG apparatus in individual pixels.

is the invariant latitude [13]) [14]. The recalculate the flux of gamma rays from the count rate (in units of photons per cm^2.s.ster) the effective area was taken from the figure displaying its dependence on energy of gamma rays [11]. For the energy range A, 0.12 - 0.32 MeV its value is 258 cm^2 and for energy range B, 3.0 - 8.3 MeV it is 213 cm^2. As for the characteristic value of the solid angle within which gamma rays are detected by SONG device $2.6 \pm 1.0\pi$ ster was used according to Ryumin et al., 1996 [8].

The values obtained from the measurement in the energy range 0.12 - 0.32 MeV have been corrected for the induced background. The procedure is described in [8]. The reason is that in the raw data there are observed the different latitudinal profiles for low and high gamma ray energies at SONG device. This is most probably caused by the fact that the significant contribution for gamma rays below 2.1 MeV is caused by the decay of the long living radioisotopes induced due to the interactions of cosmic rays with the detector material. The effect is described e.g. in Johnson et al., 1993 [15]. Since the latitudinal dependence of the induced gamma rays is practically absent [16], the induced contribution was subtracted as a constant simply from the detected gamma ray flux. The estimate of the induced gamma ray flux was done by comparison of the latitudinal dependences in the channels 0.12 - 0.32 MeV and 8.3 - 16 MeV, respectively.

4 Review of gamma ray fluxes

According to section 3 the correction for induced background was done in low energy channel. The result is seen in Figure 2 (upper panel). The lower panel of Fig. 2 is showing the distribution of high-energy gamma ray fluxes. The obtained picture should be assumed to be the combined

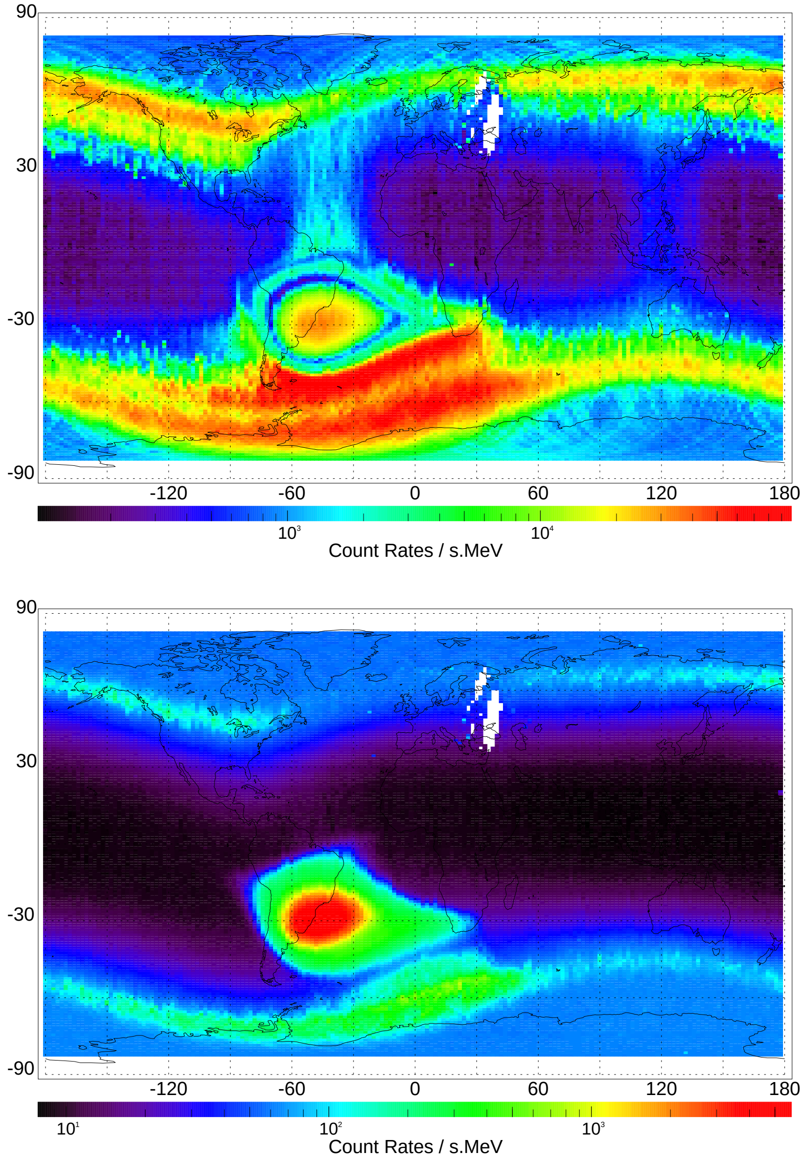

Fig. 2. The maps of average fluxes of gamma ray in energy ranges 0.12 - 0.32 MeV (upper panel) and 3.0 - 8.3 MeV (lower panel).

effect of albedo gamma rays from the Earth's atmosphere, locally produced gamma rays and of diffuse cosmic gamma ray having no latitudinal dependence.

The irregular distribution of the gamma radiation in the various geographical regions is fol-

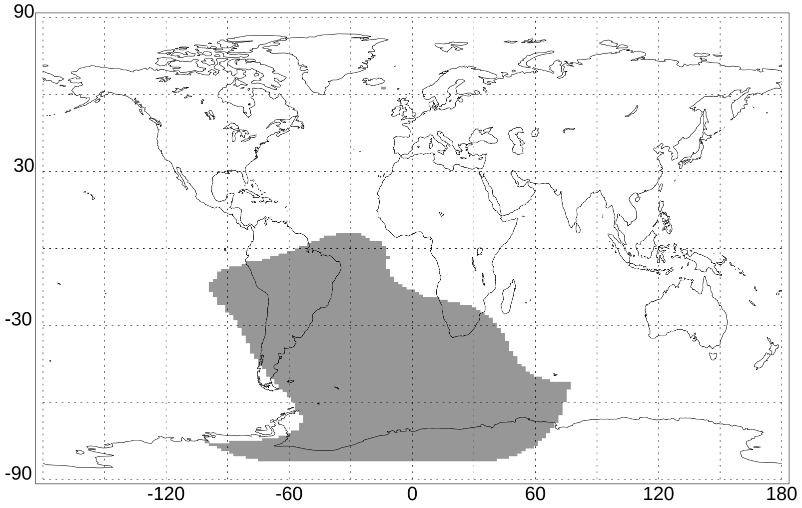

Fig. 3. Geographical position of regions where $H_{min} > 200$ km.

lowing the structure of the real magnetic field (there are anomalies in the distribution of the field strength at low altitudes) [17]. On the both panels of Figure 2, the high fluxes of gamma rays are mainly observed in the Brazilian magnetic anomaly (BMA) region $(L \sim 1.15 \div 1.8)$ and down this area $(L \sim 2.5 \div 5)$. These zones are most probably associated with particle trapped regions ($H_{min} > 200$ km, H_{min} - minimum altitude of mirror points of azimuthally drifting particles), so-called, inner and outer radiation belt. The stable trapped regions are displayed in Fig. 3.

It is seen the difference in the energy spectra (assuming the ratio of the count rate in two channels) in (a) BMA region and in (b) the gap between belts ($L \sim 1.7 \div 2.2$). In (a) rather harder spectra is seen than that in (b). It should be noted that higher energies [18] have found in the gap region between inner and outer belt significantly softer energy spectra of gamma rays than that in the inner zone. The unstable belt of energetic electrons may be formed after electron injection and their consequent radial diffusion during and after the strong magnetic disturbances [19, 20]. Such electron population can have relatively large lifetime. The high fluxes of energetic gamma rays observed in 3.0 - 8.3 MeV channel in the BMA region are probably related to the high-energy electrons and their bremsstrahlung. At energies 5 - 15 MeV and above 15 MeV, by comparison of the extent of regions of high energy proton and electron population [9] have recently suggested at 400 km the gamma rays are most probably produced by high energy electrons and not via the proton interactions with residual atmosphere and their secondaries.

Regions of precipitation of electrons from radiation belts on high latitudes and in the BMA region are clearly seen on lower panel of Fig. 2. Out of these zones flux of 3.0 - 8.3 MeV gamma rays monotonously increases with geomagnetic latitude. More complicated is upper panel of Fig. 2. Besides regions which are influenced by outer radiation belt there exist zones of high intensity

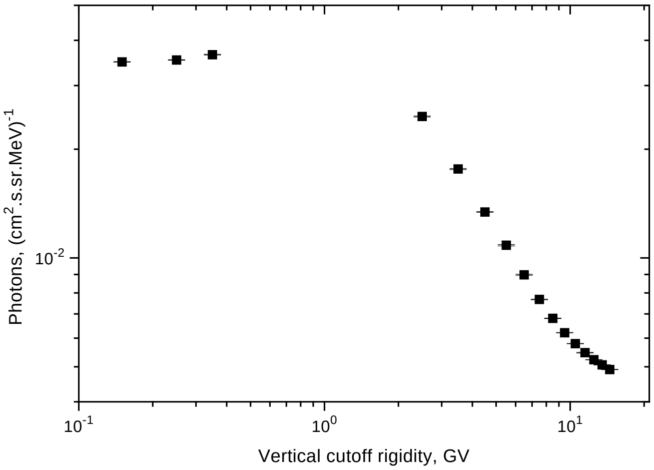

Fig. 4. Latitudinal distribution of gamma rays in the energy channel 3.0 - 8.3 MeV.

on latitudes $30^\circ \div 60^\circ$ and $-30^\circ \div -60^\circ$ and longitudes from 50° to -80°. In the BMA region instrument electronics is overloaded by a very large particle flux. To north of BMA on longitudes $-30^\circ \div -60^\circ$ up to the outer radiation belt flux is increased due to the short living radioisotopes produced in the detector matter by protons of the inner radiation belt.

Excluding the effects of trapped and quasitrapped high energy particles, the latitudinal distribution of gamma rays have been obtained. Figure 4 displays it for the channel 3.0 - 8.3 MeV. For each pixel the L and H_{min} for the position of its center have been calculated. In Fig. 4 the data are selected for those pixels, where $H_{min} < 100$ km. The vertical cut-off rigidity is computed as $R(GV) = 14.9/L^2$, the approximation of the formula (5) in the paper Shea, Smart and Gentile, 1987 [21]. Because of passages through the outer radiation belt on high latitudes there are no data for R between 0.4 GV and 2 GV. For $R > 2$ GV the power spectrum fit of the latitudinal dependence $R^{-\alpha}, \alpha = 0.94 \pm 0.03$. This is consistent with another experiments [6, 7, 8]. The preliminary estimate of the differential flux of gamma rays from 3.0 - 8.3 MeV is $(4.91 \pm 0.01) \times 10^{-3}$ and $(34.87 \pm 0.07) \times 10^{-3}$ photons/cm^2.s.sr.MeV at the equator and the pole, respectively. Obtained values are comparable to the ones from Imhof et al., 1976 [3] and Ryan et al., 1977 [22].

5 Summary

Relatively high statistics of measurements of the SONG instrument on low altitude, polar orbiting satellite CORONAS-I yielded in the obtaining of geographic distribution of gamma ray flux at 500 km in two energy intervals, namely 0.12 - 0.32 MeV and 3.0 - 8.3 MeV. At low energies the induced background has been corrected. Two features of the distribution are apparent: a - latitudinal albedo flux caused by cosmic ray primaries and having approximately 7 to 1 ratio of polar to equatorial flux comparable with others earlier experiments at different altitudes and energies, b - different energy spectra in the regions where energetic electrons being their most probable cause can be trapped, namely the inner zone with hard spectra and much softer one in the slot between the inner and outer zone.

Acknowledgement. The authors acknowledge the grant of Slovak Academy of Sciences, VEGA 2 - 5137 and SK-1. RB and KK wish to acknowledge technical assistance in computations by Mrs. J. Štetiarová.

References

[1] S.V. Golenetskiy, E.P. Mazets, V.N. Il'inskiy, R.L. Aptekar', M.M. Bredov, Yu.A. Gur'yan: *Astrophys. Lett.* **9** (1971) 69

[2] S.V. Golenetskiy, Yu.A. Gur'yan, V.N. Il'inskiy, E.P. Mazets, M.P. Proskura: *Geomagn. Aeron.* **15** (1975) 203

[3] W.L. Imhof, G.H. Nakano, J.B. Reagan: *J. Geophys. Res.* **81** (1976) 2835

[4] Yu.A. Gur'yan, E.P. Mazets, M.P. Proskura, I.A. Sokolov: *Geomagn. Aeron.* **19** (1979) 11

[5] D.J. Thomson, G.A. Simpson, M.E. Özel: *J. Geophys. Res.* **86** (1981) 1265

[6] Yu.E. Efimov, A.A. Gusev, K. Kudela, L. Just, G.I. Pugacheva: *Czech. J. Phys. B* **35** (1985) 1371

[7] D.J. Forrest: *AIP Conf. Proc. 186 High Energy Radiation Background in Space,* eds. A.C. Rester, J.I. Trombka, New York, 1989, p. 243;

[8] S.P. Ryumin, A.V. Bogomolov, A.V. Dmitriev, I.N. Myagkova: *J. Moscow Phys. Soc.* **6** (1996) 423

[9] A.V. Bogomolov, V.V. Bogomolov, Yu.I. Denisov, G.Ya. Kolesov, Yu.I. Logachev, S.I. Svertilov, M.I. Kudryavtsev, V.M. Pankov: 25^{th} *International Cosmic Ray Conference vol. 2.,* eds. M.S. Potgieter, B.C. Raubenheimer and D.J. van der Walt, Potchefstroomse Universiteit, Durban, 1997, p. 337;

[10] I.M. Martin, S.L.G. Dutra, R.A. Palmeira: *Revista Brasileira de Física* **5** (1975) 43

[11] J. Baláž, A.V. Dmitriev, M.A. Kovalevskaya, K. Kudela, S.N. Kuznetsov, I.N. Myagkova, Yu.I. Nagornikh, J. Rojko, S.P. Ryumin: *IAU Colloq. 144 "Solar Coronal Structures",* eds. V. Rušin, P. Heinzel and J.-C. Vial, VEDA, Bratislava, 1994, p. 635;

[12] R. Bučík, K. Kudela, A.V. Bogomolov, I.N. Myagkova, S.N. Kuznetsov, S.P. Ryumin: *Contrib. Astron. Obs. Skalnaté Pleso* **29** (1999) 147

[13] J.G. Roederer: *Dynamics of Geomagnetically Trapped Radiation*, Springer-Verlag, New York, 1970.

[14] S.N. Kuznetsov, A.V. Bogomolov, A.V. Dmitriev, K. Kudela, I.N. Myagkova, S.P. Ryumin: *Izv. Russian Acad. Sci., ser. phys.* **6** (1997) 1104

[15] W.N. Johnson, R.L. Kinzer, J.D. Kurfess, M.S. Strickman, W.R. Purcell, D.A. Grabelsky, M.P. Ulmer, D.A. Hillis, G.V. Jung, R.A. Cameron: *Astrophys. J. Suppl.* **86** (1993) 693

[16] A.J. Dean, F. Lei, P.J. Knight: *Space Sci. Rev.* **57** (1991) 109

[17] S.N. Vernov, E.V. Gorchakov, P.I. Shavrin, K.N. Sharvina: *Space Sci. Rev.* **7** (1967) 490

[18] A.M. Galper, S.V. Koldashev, L.V. Maslennikov, V.V. Mikhailov, N.I. Schvetz, S.A. Voronov: 25^{th} *International Cosmic Ray Conference vol. 2.,* eds. M.S. Potgieter, B.C. Raubenheimer and D.J. van der Walt, Potchefstroomse Universiteit, Durban, 1997, p. 333;

[19] J.B. Blake, W.A. Kolasinski, R.W. Fillius, E.G. Mullen: *Geophys. Res. Lett.* **19** (1992) 821

[20] Li. Xinlin, I. Roth, M. Temerin, J.R. Wygant, M.K. Hudson, J.B. Blake: *Geophys. Res. Lett.* **20** (1993) 2423

[21] M.A. Shea, D.F. Smart, L.C. Gentile: *Phys. of the Earth and Planet. Interiors* **48** (1987) 200

[22] J.M. Ryan, B. Dayton, S.H. Moon, R.B. Wilson, A.D. Zych, R.S. White: *J. Geophys. Res.* **82** (1977) 3593